

## Primary and secondary modes of deformation twinning in HCP Mg based on atomistic simulations

Hong-lu XU<sup>1</sup>, Xiao-ming SU<sup>2</sup>, Guang-yin YUAN<sup>1,2</sup>, Zhao-hui JIN<sup>2</sup>

1. National Engineering Research Center for Light Alloy Net-Forming, Shanghai Jiao Tong University, Shanghai 200240, China;
2. School of Materials Science and Engineering, Shanghai Jiao Tong University, Shanghai 200240, China

Received 17 October 2013; accepted 5 November 2014

**Abstract:** Deformation twinning, i.e., twin nucleation and twin growth (or twin boundary migration, TBM) activated by impinged basal slip at a symmetrical tilt grain boundary in HCP Mg, was examined with molecular dynamics (MD) simulations. The results show that the  $\{\bar{1}\bar{1}21\}$ -type twinning acts as the most preferential mode of twinning. Once such twins are formed, they are almost ready to grow. The TBM of such twins is led by pure atomic shuffling events. A secondary mode of twinning can also occur in our simulations. The  $\{11\bar{2}2\}$  twinning is observed at 10 K as the secondary twin. This secondary mode of twinning shows different energy barriers for nucleation as well as for growth compared with the  $\{\bar{1}\bar{1}21\}$ -type twinning. In particular, TBMs in this case is triggered intrinsically by pyramidal slip at its twin boundary.

**Key words:** magnesium; atomistic simulation; deformation twinning; twin boundary migration; dislocation-grain boundary interaction

### 1 Introduction

Magnesium and its alloys have been widely applied in many areas, especially attractive for automotive and aerospace applications [1]. As a typical ultra-lightweight material, it has extraordinarily properties such as low density ( $\sim 1.74 \text{ g/cm}^3$ ), high specific strength and stiffness, good high temperature mechanical properties, and outstanding recyclability [2]. The deformation of magnesium is very complex because of its hexagonal close-packed (HCP) structure with low crystal symmetry [3,4]. Thus, it often exhibits poor ductility and the plastic deformation mechanisms of Mg are not clearly understood. However, there are many twinning activities due to the limited number of slip systems for dislocation glide. For this reason, twinning is an important deformation mechanism in Mg alloys [5–8].

There are four major twinning modes related to plastic deformation:  $\{10\bar{1}1\}\langle 10\bar{1}2 \rangle$ ,  $\{10\bar{1}2\}\langle 10\bar{1}1 \rangle$ ,  $\{11\bar{2}1\}\langle 11\bar{2}6 \rangle$  and  $\{11\bar{2}2\}\langle 11\bar{2}3 \rangle$ . To understand the mechanical behaviors of the Mg and its alloys, we aim to

reveal atomic level mechanisms of deformation twinning. In particular, we pay our attention to the nucleation of micro-twins due to interaction between dislocation and grain boundary and the subsequent growth of micro-twin.

Currently, much effort has been put into the mechanisms explanation of twin nucleation and growth in Mg, especially two dominant twinning modes,  $\{10\bar{1}1\}\langle 10\bar{1}2 \rangle$  and  $\{10\bar{1}2\}\langle 10\bar{1}1 \rangle$ , with  $\{10\bar{1}2\}\langle 10\bar{1}1 \rangle$  being mentioned as the most common mode. Atomistic simulations are greatly used in this area [9–20].

WANG et al [13,14] proposed that the twin nucleation and growth were due to the movement of twinning dislocations on their twinning planes. They confirm the twin nucleation by pure shuffle mechanism and explain the growth of a twin by glide-shuffle mechanism [10–12]. As a result, the  $\{10\bar{1}2\}$  twinning mode is the most common one for researches of twinning nucleation and growth. And there is controversy about the mechanism of twin nucleation and growth. However, in our simulations, two other twinning modes of the four major modes,  $\{11\bar{2}1\}$  and  $\{11\bar{2}2\}$ , were examined. The

molecular dynamics simulation results are hopefully useful to further clarify some twinning-related phenomena.

## 2 Methods

The sample consisted of multiple overlapping units along three orthogonal directions, as shown in Fig. 1(a). The unit was a rhomb containing  $e_1$ ,  $e_2$  and  $e_3$ , as shown in Fig. 1(b). The sample contained a symmetry tilt grain boundary (GB).  $(\bar{1}\bar{1}23)$  plane was chosen as the GB plane and the tilt angle  $\theta$  of basal planes is  $47.2^\circ$  (see Fig. 1(c)). The sample had two free surfaces in the  $z$  direction perpendicular to the GB normal. Periodic boundary conditions were used in both  $x$  and  $y$  directions so the sample represented a free-standing thin-film of “bicrystal” with a GB in between. A crack tip was introduced on one surface of the sample. The crack tip was used as a dislocation source when the slab was under

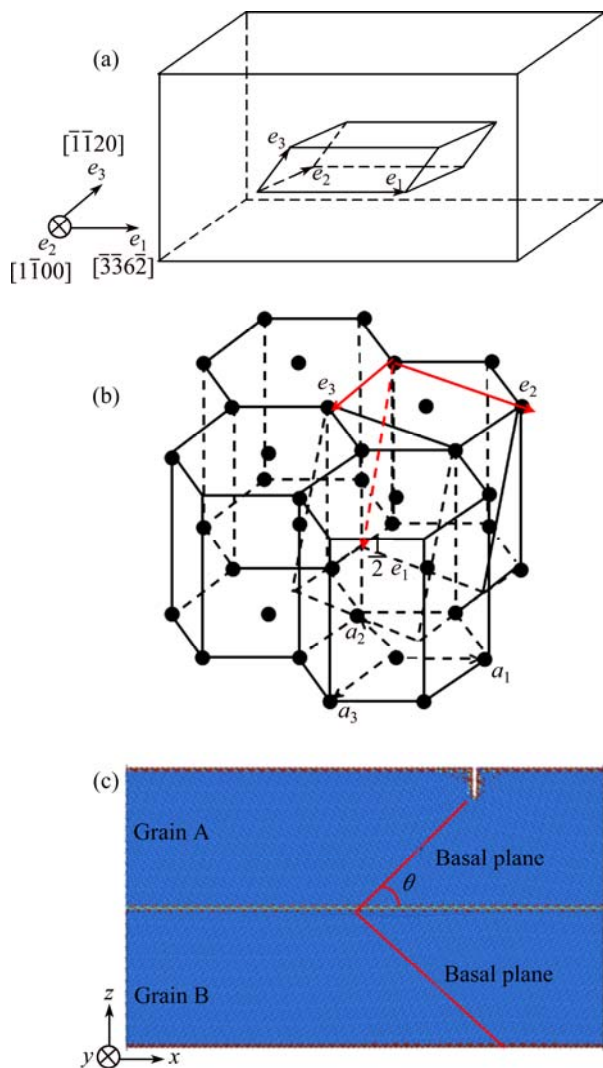


**Fig. 1** Sample description and simulation model building process: (a) Simulation model; (b) Atomic model; (c) Overall model for atomic simulation

tensile loading. The samples were prepared by full relaxation at chosen temperatures (10 K in our case) in NPT ensemble using Nöse–Hoover algorithm with the MD codes LAMMPS. The sample was deformed by applying a homogeneous tensile strain in  $x$  direction at a constant rate of  $10^8 \text{ s}^{-1}$ . The MD time step was set to be 2.5 fs throughout this work. LEE’s potential was used to model the HCP metal Mg. Such MEAM potential was a modified one with angular dependence, and it has been widely used to study twin structures, deformation twinning and dislocation reactions.

## 3 Observations

In the MD simulations, the sample was subjected to tensile loading in the  $x$  ( $e_1$ ) direction. A low temperature was chosen for the experiment. The experiment was carried out at 10 K and the loading rate was  $10^8 \text{ s}^{-1}$ , the ensemble was minimization.

### 3.1 Interactions between dislocations and grain boundary

Figure 2 shows the change of stress with applied strain along the  $x$  direction. With the increase of stress, dislocations are emitted from the crack tip and release concentrated stress there [21]. The interactions between dislocations and the symmetric tilt grain boundary can lead to twin nucleation at a certain applied stress [22]. From our simulation model, at 10 K temperature, the critical stress of dislocation emission from the crack tip is 1.443 GPa at point  $A$  (corresponding to Fig. 3(a)) in Fig. 2. When a dislocation is generated, the applied stress of this sample could be released and then continue to increase. The perfect dislocation moves along the basal plane and interacts with the symmetric tilt grain boundary. After four perfect dislocations are generated and interact with the pre-existed grain boundary, twin nuclei are formed at the interacting area with the highest 1.664 GPa stress at point  $B$  (corresponding to Fig. 3(b)). As long as a twin is nucleated, the stress decreases rapidly to point  $C$ , 0.0743 GPa. This means that the twin nucleation can release the stress of the sample and lead to better deformation. After a primary twin is nucleated, the applied stress continues to increase and the twin grows. The emission of twinning dislocations from interactions between dislocations and grain boundary at each of the twin boundaries changes the direction of twinning planes, and there is an obvious rise of stress with the primary twin growth, so twin growth has a strengthening effect. With increasing stress and the changing orientation relationship from primary twin nucleation and growth, a secondary twin is nucleated later to better support the further deformation of the sample.

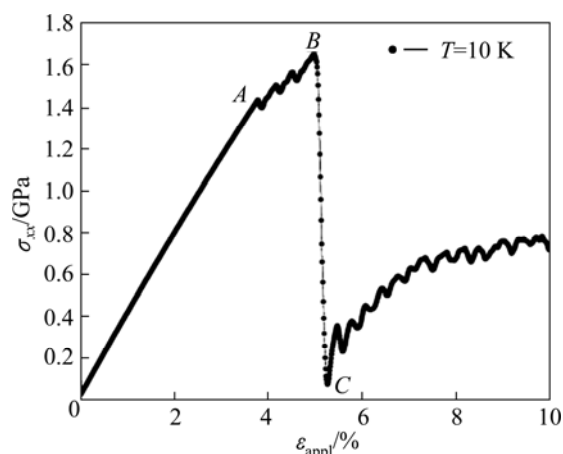


**Fig. 2** Changes of stress with applied strain along  $x$  direction

We can observe the primary and secondary twins clearly in Fig. 3. It contains different stages of the sample corresponding to different applied strains in Fig. 2. These dislocations glide on basal plane and will impinge at the grain boundary one by one (see Fig. 3(a)). Impinging dislocations lead to the generation of twin dislocations due to the interaction of glide dislocations with the grain boundary. Four dislocations are enough to nucleate a twin (see Fig. 3(b)) at 10 K temperature. In the meantime of twin nucleation, the stress decreases substantially because twin nucleation can release the stress of the sample to a certain degree. This first primary twin is  $\{\bar{1}\bar{1}21\}$  twin. With the growth of primary twin, many steps appear at the bottom of sample from the deformation caused by  $\{\bar{1}\bar{1}21\}$  twin. Many partial dislocations are gathering together at the tip of this micro-twin. During this process, stress of grain  $A$  can be released by dislocation emission and transferred at the same time from grain  $A$  to grain  $B$  by twin nucleation at the grain boundary. When penetrating grain  $B$ , this twin grows wider under increasing stress (see Fig. 3(c)). And a secondary twin  $\{\bar{1}\bar{1}22\}$  is activated from these steps. Also, primary  $\{\bar{1}\bar{1}21\}$  twin growth makes the under surface of grain  $B$  deform severely, in this way, there are many steps which can be regarded as another dislocation source along the deformed area. When the primary twin grows to a certain degree, these steps turn into dislocations to form a secondary twin (see Fig. 3(d)). Then, with the growth of this twin, stress increases. And the secondary twin  $\{\bar{1}\bar{1}22\}$  is activated by the steps on the surface.

Simulation results show that a slip dislocation can undergo a core reconstruction or dissociate into interfacial defects when meeting a particular grain boundary. The mechanisms of twinning nucleation and growth at 10 K can be explained by the generation and gliding of twinning dislocation and atomic shuffling around the twin boundary. Perfect dislocations emission

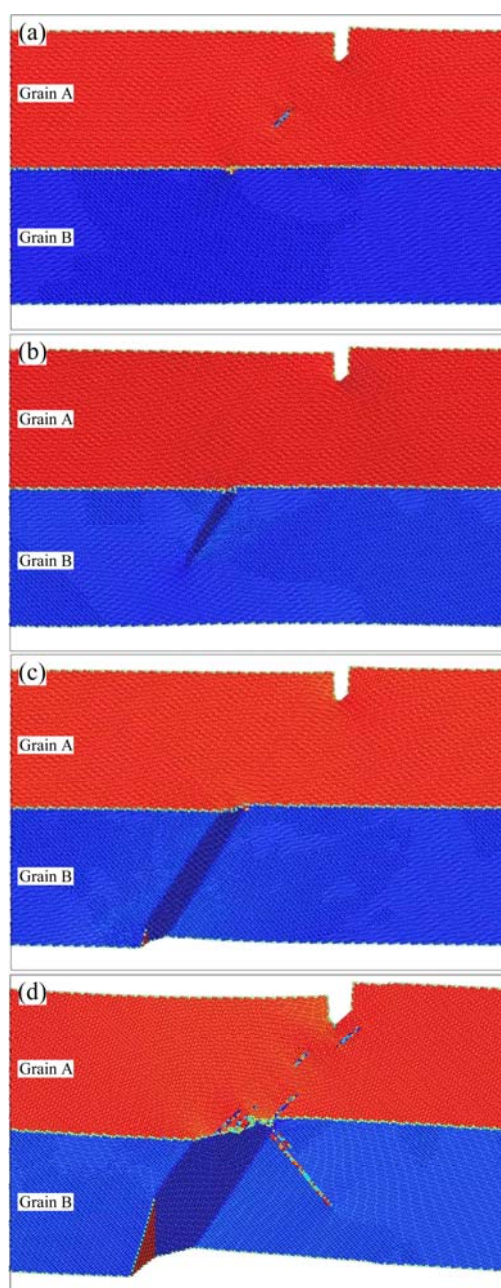


**Fig. 3** Dislocations interacting with grain boundary leading to twinning nucleation and growth: (a)  $\varepsilon_{xx}=4.867\%$ ,  $\sigma_{xx}=1.634$  GPa; (b)  $\varepsilon_{xx}=4.113\%$ ,  $\sigma_{xx}=0.864$  GPa; (c)  $\varepsilon_{xx}=6.446\%$ ,  $\sigma_{xx}=0.523$  GPa; (d)  $\varepsilon_{xx}=8.992\%$ ,  $\sigma_{xx}=0.765$  GPa

comes from the crack tip along the  $[11\bar{2}0]$  direction of grain  $A$ . Then, this dislocation interacts with the grain boundary and dissociates into a partial dislocation and a twinning dislocation.

As a result  $\{\bar{1}\bar{1}21\}$  twin appears as the primary twin while  $\{\bar{1}\bar{1}22\}$  is the secondary twin. To explain this result, we should further study the twin boundary migrations. Because the twin nucleation could not decide whether this twin can finally be formed. It is decided by the movement of twin boundary which can release the energy.

### 3.2 Mechanism of twin boundary migrations

The twin boundary models of  $\{\bar{1}\bar{1}21\}$  primary twin and  $\{\bar{1}\bar{1}22\}$  secondary twin were built to analyze the methods and difficulties of twin boundary migrations, as shown in Fig. 4. Tensile loading stress was applied along the  $x$  direction to make the twin boundary migrate. In this way, we can observe and analyze their migration mechanisms and explain the difficulties for their formations.

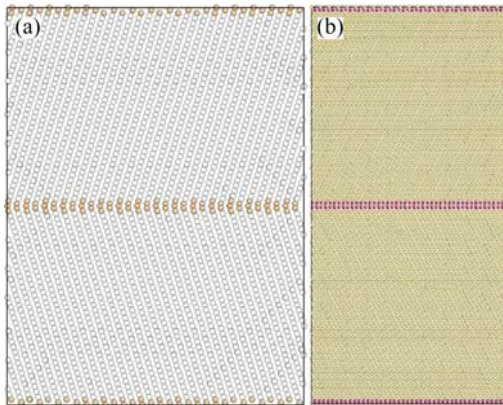


**Fig. 4** Twin boundary migration models: (a)  $\{\bar{1}\bar{1}21\}$  primary twin migration model; (b)  $\{\bar{1}\bar{1}22\}$  secondary twin migration model

The stress–strain curves in Fig. 5 show the migration process for two types of twins. After the stress increases to the highest point to activate the twin boundary migration, it falls rapidly to the lowest point and the stress releases. And then the stress continues to increase to activate another twin boundary migration. Such process happens repeatedly with the stress going up and down. From the stress curves, it can be seen that the  $\{\bar{1}\bar{1}21\}$  twin boundary is easier to migrate for it has a very low activating stress compared with  $\{\bar{1}\bar{1}22\}$  twin boundary. And once  $\{\bar{1}\bar{1}21\}$  twin boundary is activated to migrate, it moves very fast to release its stress. This may explain in a way that why  $\{\bar{1}\bar{1}21\}$  appears as the primary twin, and  $\{\bar{1}\bar{1}22\}$  is activated after the primary one. However, to better explain the difficulties to activate and form a twin, the mechanism of these twin boundary migrations should be discussed.

The  $\{\bar{1}\bar{1}21\}$  twin boundary migration is explained by the pure-shuffle mechanism. Figures 6(c) and (d) shows the detailed part of Figs. 6(a) and (b) which represents one migration process for this twin boundary. The atoms marked in black lines are the same series in Fig. 6(c). We can see that once the grain boundary migrates, atoms at twin boundary just need to move very little to adjust their places and in this way complete the migration. We regard this process as pure-shuffle. The atomic shuffling occurs and is easily completed for it needs low energy to drive.

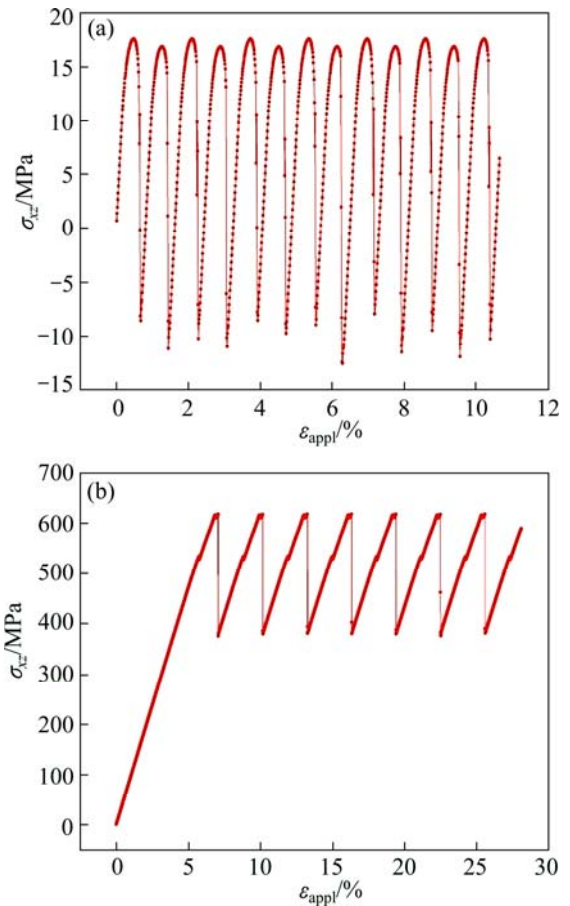


**Fig. 5** Stress–strain curves of three types of twin boundary migrations: (a) For  $\{\bar{1}\bar{1}21\}$ ; (b) For  $\{\bar{1}\bar{1}22\}$

The mechanism of  $\{\bar{1}\bar{1}22\}$  twin boundary migration is because of the  $\langle a+c \rangle$  dislocation type. Figure 7 shows the migration process of atoms at the twin boundary. Also, the atoms marked in black lines are the same series during one migration. When the red atoms of upper row change to the lower line, they experience dislocations along  $[22\bar{4}3]$  and  $[\bar{1}\bar{1}20]$  directions. The movement locus of those atoms in twinning boundary is a zigzag way. Two successive movements of each directions form a direct displacement along the  $[11\bar{2}3]$  direction which is regarded as the type of pyramidal  $\langle a+c \rangle$  slip. As a result, we can see that the  $\{\bar{1}\bar{1}22\}$  twin boundary migration is more complex than the  $\{\bar{1}\bar{1}21\}$  primary twin boundary migration. To accomplish the secondary twin boundary migration, they need to complete two types of dislocations along two directions as the pyramidal slip. This needs higher energy and stress to activate the migration.

From the two migration models, the twin boundary migrations of primary and secondary twin are clearly observed. And the reason for  $\{\bar{1}\bar{1}21\}$  as the primary twin is because the mechanism of its twin boundary migration is pure-shuffle. This is an easily activated process during the migration. And the  $\{\bar{1}\bar{1}22\}$  twin

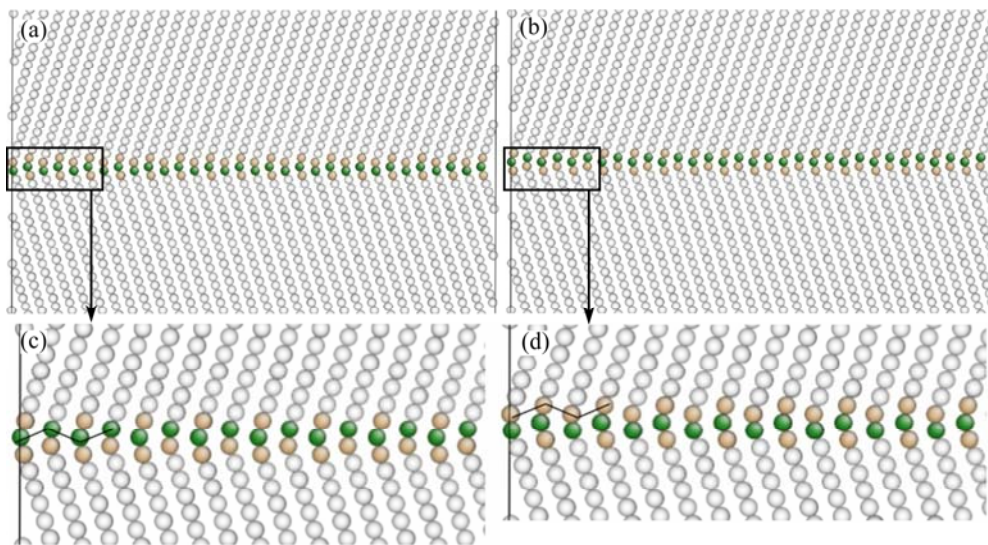


**Fig. 6**  $\{\bar{1}\bar{1}21\}$  twin boundary migration (a), description of process of atomic shuffling (b) and detailed part (c, d) for (a) and (b)

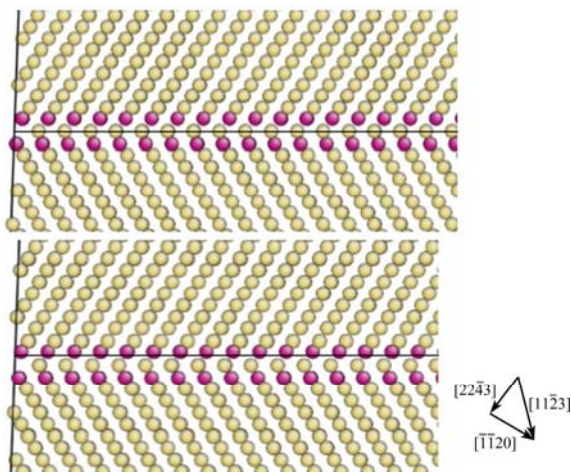


**Fig. 7**  $\{\bar{1}\bar{1}22\}$  twin boundary migration

boundary migration needs higher stress and energy, and is accomplished by pyramidal slip. This process needs higher stress and energy, and experiences a complex mechanism for twin boundary migration. As a result, the  $\{\bar{1}\bar{1}21\}$  twin is activated and formed as the primary twin and a secondary twin of  $\{\bar{1}\bar{1}22\}$  is produced afterwards.

## 4 Conclusions

1) The  $\{\bar{1}\bar{1}21\}$  primary twin boundary migration can be explained by pure-shuffle process while the secondary twin boundary migration of  $\{\bar{1}\bar{1}22\}$  is accomplished by the pyramidal slip.

2) The mechanisms of the twin boundary migration can better explain the priority for the twins in the simulation.

3) The twin nucleation and growth can be explained by atomic shuffling and glide-shuffle mechanisms.

## References

- [1] YANG Li-wen, ZHANG Yan, LI Jun, LI Yun, ZHONG Jian-xin, CHU P K. Magnetic and upconverted luminescent properties of multifunctional lanthanide doped cubic KGdF<sub>4</sub> nanocrystals [J]. *Nanoscale*, 2010, 2(12): 2805–2810.
- [2] FRIEDRICH H E, MORDIKE B L. Magnesium technology: Metallurgy, design data, automotive applications [M]. Berlin: Springer, 2006.
- [3] MATSUZUKI M, HORIBE S. Analysis of fatigue damage process in magnesium alloy AZ31 [J]. *Materials Science and Engineering A*, 2009, 504(1): 169–174.
- [4] MURRAY S J, MARIONI M, ALLEN S M, O'HANDLEY R C, LOGRASSO T A. 6% magnetic-field-induced strain by twin-boundary motion in ferromagnetic Ni–Mn–Ga [J]. *Appl Phys Lett*, 2000, 77: 886–888.
- [5] MOLNAR P, JAGER A, LEJCEK P. Twin nucleation at grain boundaries in Mg–3wt.% Al–1wt.% Zn alloy processed by equal channel angular pressing [J]. *Scripta Mater*, 2012, 67(5): 467–470.
- [6] WANG J, BEYERLEIN I J. Atomic structures of symmetric tilt grain boundaries in hexagonal close-packed (hcp) crystals [J]. *Metall Mater Trans A*, 2012, 43(10): 3556–3569.
- [7] WANG J, BEYERLEIN I J, HIRTH J P. Nucleation of elementary  $\{1\bar{0}11\}$  and  $\{1\bar{0}13\}$  twinning dislocations at a twin boundary in hexagonal close-packed crystals [J]. *Model Simul Mater Sc*, 2012, 20(2): 024001
- [8] WANG J, HOAGLAND R G, HIRTH J P, CAPOLUNGO L, BEYERLEIN I J, TOMÉ C N. Nucleation of a  $\{1\bar{0}12\}$  twin in hexagonal close-packed crystals [J]. *Scripta Mater*, 2009, 61(9): 903–906.
- [9] WANG J, HIRTH J P, TOMÉ C N.  $\{1\bar{0}12\}$  twinning nucleation mechanisms in hexagonal-close-packed crystals [J]. *Acta Mater*, 2009, 57(18): 5521–5530.
- [10] WANG Jing-tao, YIN De-liang, LIU Jin-qiang, TAO Jun, SU Yan-ling, ZHAO Xiang. Effect of grain size on mechanical property of Mg–3Al–1Zn alloy [J]. *Scripta Mater*, 2008, 59(1): 63–66.
- [11] WANG Jian, JIANG Bing, DING Pei-dao, PAN Fu-sheng, DAI Yong-gang. Study on solidification microstructure of AZ31 alloy strips by vertical twin roll casting [J]. *Materials Science Forum*, 2007, 546–549: 383–386.

- [12] LI B, MA E. Atomic shuffling dominated mechanism for deformation twinning in magnesium [J]. *Phys Rev Lett*, 2009, 103(3): 035503.
- [13] LI B, MA E. Pyramidal slip in magnesium: Dislocations and stacking fault on the  $\{10\bar{1}1\}$  plane [J]. *Philos Mag*, 2009, 89(14): 1223–1235.
- [14] LI B, MA E. Li and Ma reply [J]. *Phys Rev Lett*, 2010, 104(2): 029604.
- [15] SARKER D, CHEN D. Detwinning and strain hardening of an extruded magnesium alloy during compression [J]. *Scripta Mater*, 2012, 67(2): 165–168.
- [16] BEYERLEIN I, WANG J, BARMETT M, TOME C. Double twinning mechanisms in magnesium alloys via dissociation of lattice dislocations [J]. *Proceedings of the Royal Society A: Mathematical, Physical and Engineering Science*, 2012, 468(2141): 1496–1520.
- [17] LU Lei, SHEN Yong-feng, CHEN Xian-hua, QIAN Li-hua, LU Ke. Ultrahigh strength and high electrical conductivity in copper [J]. *Science*, 2004, 304(5669): 422–426.
- [18] ONO N, NOWAK R, MIURA S. Effect of deformation temperature on Hall-Petch relationship registered for polycrystalline magnesium [J]. *Mater Lett*, 2004, 58(1–2): 39–43.
- [19] SHAO X H, YANG Z Q, MA X L. Strengthening and toughening mechanisms in Mg–Zn–Y alloy with a long period stacking ordered structure [J]. *Acta Mater*, 2010, 58(14): 4760–4771.
- [20] HENKELMAN G, JONSSON H. Improved tangent estimate in the nudged elastic band method for finding minimum energy paths and saddle points [J]. *Journal of Chemical Physics*, 2000, 113: 9978–9985.
- [21] BLOCHL P E. Projector augmented-wave method [J]. *Phys Rev B*, 1994, 50(24): 17953–17979.
- [22] METHFESSEL M, PAXTON A T. High-precision sampling for Brillouin-zone integration in metals [J]. *Phys Rev B*, 1989, 40(6): 3616–3621.

## 基于原子尺度模拟研究 HCP 镁中的一次及二次孪生模式

徐泓鹭<sup>1</sup>, 苏小明<sup>2</sup>, 袁广银<sup>1,2</sup>, 金朝晖<sup>2</sup>

1. 上海交通大学 轻合金成型国家工程研究中心, 上海 200240;
2. 上海交通大学 材料科学与工程学院, 上海 200240

**摘要:** 通过分子动力学模拟(MD), 研究在 HCP 镁中的一个对称倾斜晶界与基面滑移的位错相互作用而激发的变形孪晶, 也就是孪晶形核与长大的过程(或者是孪晶界迁移, TBM)。 $\{\bar{1}\bar{1}21\}$  孪晶在该过程中是最易被激发的孪生模式。一旦这样的孪晶形成了, 它们就会不断长大。该种孪晶界迁移是由单纯的原子位置局域调整造成的。在模拟过程中同时也产生了二次孪晶  $\{\bar{1}\bar{1}22\}$ 。该二次孪晶模型的孪晶形核与长大需要克服的能垒与  $\{\bar{1}\bar{1}21\}$  孪晶不同。同时, 二次孪晶的孪晶界迁移过程是通过孪晶界上的锥形滑移而激发的。

**关键词:** 镁; 原子模拟; 变形孪晶; 孪晶界迁移; 位错-晶界相互作用

(Edited by Yun-bin HE)